

Is there a tropical response to recent observed Southern Ocean cooling?

Xiyue Zhang¹, Clara Deser¹, and Lantao Sun²

¹National Center for Atmospheric Research, Boulder, Colorado, USA

²Colorado State University, Fort Collins, Colorado, USA

Contents of this file

Text S1

Figures S1 to S6

Introduction

This supporting information provides description of our observational data sets, analysis methods, mixed layer budget equations and figures that are complementary to the main article.

Text S1.

Observational Data Sets

We use a suite of data sets to capture the observed trends during 1979-2013. SSTs are taken from the NOAA ERSSTv3b data set with 2° global resolution (Smith et al., 2008), for compatibility with those used in TPACE and SOPACE. We also show the SO SST anomaly timeseries from ERSSTv5 data set for comparison (Huang et al., 2017). The two data sets don't show significant differences in their SO SST trends (Figure S1). Surface wind data are taken from ERA-5 Reanalysis at 0.25° global resolution (Hersbach et al., 2019). Sea ice concentration data are from the passive-microwave-derived NASA Goddard Bootstrap version 2 dataset on a 25 km x 25 km grid (Peng et al., 2013).

Analysis Methods

We calculate monthly anomalies of all fields by subtracting the climatological monthly means of the 1981-2010 base period. Linear least-square regression is used to compute monthly trends during 1979-2013. We use stippling to indicate regions of statistical significance at 95% confidence level, based on a two-sided t -test method adjusted for autocorrelation (Santer et al., 2000; Schneider & Deser, 2018).

Ocean Mixed Layer Budget Equations

We focus on the ensemble-mean ocean mixed layer budget in SOPACE-internal, in order to isolate the forced response to the internal component of observed SO SST trends. The surface mixed-layer budget equation is:

$$\rho c_p H \frac{\partial T_s}{\partial t} = F_{SW} + F_{LW} + SH + LH + O. \quad (S1)$$

We can take the linear trend of Equation S1, the left-hand side which represents the trend of heat storage is negligible (Cook et al. 2018, also see Figure S3b), we will have

$$0 = F_{SW}^t + F_{LW}^t + SH^t + LH^t + O^t, \quad (S2)$$

where the superscript t denotes *linear trends* during 1979-2013.

Figure S3 shows all terms in Equation S3. The sensible heat flux trend is the smallest term. The rest of the terms can be considered forcing on SST trend T_s^t due to clouds (F_{SW}^t), ocean dynamics (O^t), and atmospheric temperature and humidity (F_{LW}^t). The latent heat flux term directly depends on T_s via saturation vapor pressure:

$$LH = -L_v c_E \rho_a W [q_s(T_s) - q_a]. \quad (S3)$$

And q_a is the specific humidity of air above the sea surface, thus can be written as

$$q_a = RH_0 q_s(T_s + \Delta T), \quad (S4)$$

where RH_0 is the relative humidity at the sea surface, and $\Delta T = T_a - T_s$ is the temperature gradient near the sea surface. Using the Clausius-Clapeyron equation, Equation S4 can be written as

$$q_a = RH_0 q_s(T_s) e^{\alpha \Delta T}, \quad (S5)$$

Where $\alpha = \frac{L_v}{R_v T^2} \approx 0.06 \text{ K}^{-1}$. We can plug Equation S5 into S3 and get

$$LH = -L_v c_E \rho_a W (1 - RH_0 e^{\alpha \Delta T}) q_s(T_s)$$

Following Hwang et al. (2017) and Jia & Wu (2013), the linear trend of latent heat flux can therefore be linearized as

$$LH^t = \frac{\partial LH}{\partial T_s} T_s^t + \frac{\partial LH}{\partial W} W^t + \frac{\partial LH}{\partial RH_0} RH_0^t + \frac{\partial LH}{\partial \Delta T} \Delta T^t \quad (S6)$$

On the right-hand side (RHS), the last three terms can also be considered as forcing from the atmosphere due to changes in near-surface wind speed, near-surface relative humidity, and air-sea temperature gradient:

$$LH_W^t = \frac{\partial LH}{\partial W} W^t = \overline{LH} \frac{W^t}{\overline{W}}, \quad (S7)$$

$$LH_{RH}^t = \frac{\partial LH}{\partial RH_0} RH_0^t = -\frac{\overline{LH} RH_0^t}{e^{\alpha \Delta T} - \overline{RH_0}}, \quad (S8)$$

$$LH_{\Delta T}^t = \frac{\partial LH}{\partial \Delta T} \Delta T^t = \frac{\alpha \overline{LH} \overline{RH_0} \Delta T^t}{e^{\alpha \Delta T} - \overline{RH_0}}, \quad (S9)$$

while the first term on RHS of Equation S6 becomes the SST damping term:

$$\frac{\partial LH}{\partial T_s} T_s^t = \alpha \overline{LH} T_s^t, \quad (S10)$$

where \overline{LH} is the climatological mean latent heat flux, and it is negative when evaporation happens. This term in Equation S10 means that higher SST evaporates more to cool, therefore damps the temperature change. Equation S10 allows us to rewrite Equation S2 as a diagnostic equation of the SST trend:

$$T_s^t = -\frac{F_{SW}^t + F_{LW}^t + SH^t + O^t + LH_W^t + LH_{RH}^t + LH_{\Delta T}^t}{\alpha \overline{LH}}. \quad (S11)$$

We can rewrite Equation S11 to show how different forcing terms contribute to the SST trends:

$$T_s^t = T_{SW}^t + T_{LW}^t + T_{SH}^t + T_O^t + T_{LH,W}^t + T_{LH,RH}^t + T_{LH,\Delta T}^t, \quad (S12)$$

where the RHS terms can be defined using Equation S7–S9.

$$T_{SW}^t = -\frac{F_{SW}^t}{\alpha \overline{LH}}, \quad (S13)$$

$$T_{LW}^t = -\frac{F_{LW}^t}{\alpha \overline{LH}}, \quad (S14)$$

$$T_{SH}^t = -\frac{F_{SH}^t}{\alpha \overline{LH}}, \quad (S15)$$

$$T_O^t = -\frac{F_O^t}{\alpha \overline{LH}}, \quad (S16)$$

$$T_{\text{LH,w}}^t = -\frac{LH_{\text{w}}^t}{\alpha \overline{LH}} = -\frac{W^t}{\alpha \overline{W}}, \quad (\text{S17})$$

$$T_{\text{LH,RH}}^t = -\frac{LH_{\text{RH}}^t}{\alpha \overline{LH}} = \frac{RH_0^t}{\alpha(e^{\alpha \overline{\Delta T}} - \overline{RH_0})}, \quad (\text{S18})$$

$$T_{\text{LH},\Delta T}^t = -\frac{LH_{\Delta T}^t}{\alpha \overline{LH}} = -\frac{\overline{RH_0}}{e^{\alpha \overline{\Delta T}} - \overline{RH_0}} \Delta T^t. \quad (\text{S19})$$

Equation S12–S19 are shown in Figure 2, while the heat flux trend terms used to calculate Equation S12–S19 are shown in Figure S3.

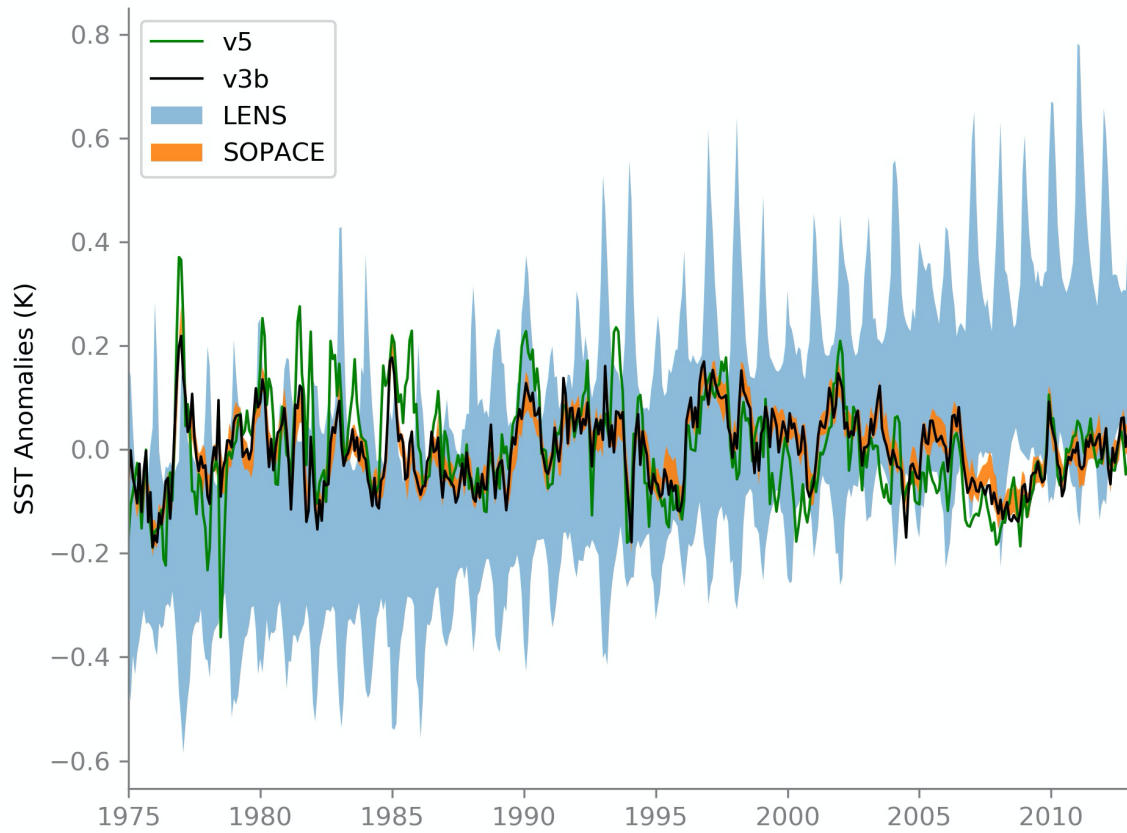


Figure S1. Southern Ocean (40-65S) averaged monthly SST anomaly from SOPACE (orange shading), LENS (blue shading), ERSSTv3b dataset (black), and ERSSTv5 (green). The 1975-2016 climatology is used to calculate the monthly anomaly.

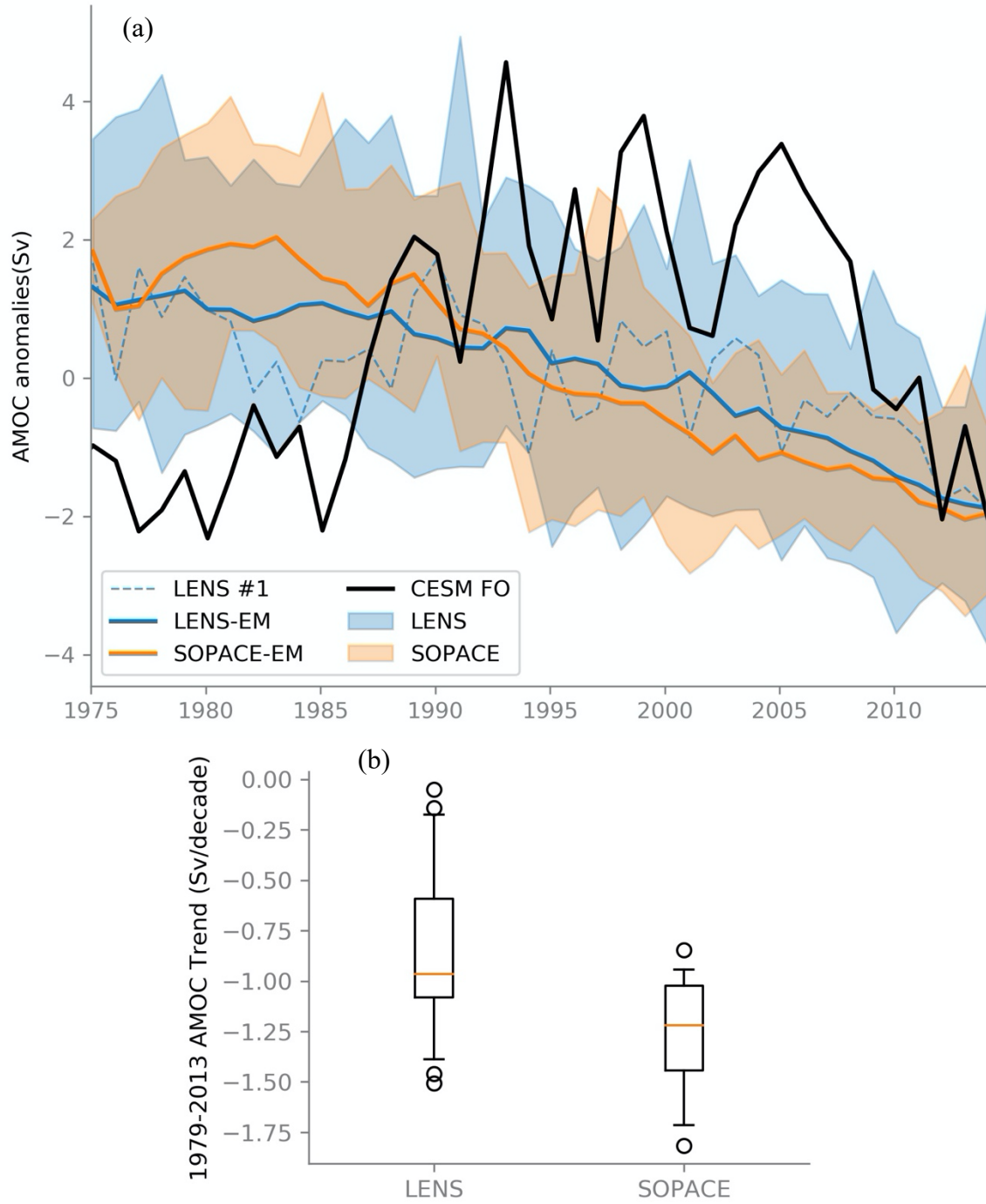


Figure S2. (a) Annual mean AMOC anomaly timeseries (defined as the maximum streamfunction value in the latitude band 20–60N and below 500 m in the Atlantic Ocean following Zhang et al. 2017). The black line shows the CESM forced ocean (FO) simulation (Yeager et al. 2018), approximating the observed AMOC timeseries. Blue solid curve shows the ensemble mean of LENS, with blue shading showing the range of the ensemble spread. Orange solid curve shows the ensemble mean of SOPACE, with orange shading showing the range of the ensemble spread. The dashed blue curve

shows the first ensemble member of LENS, which was used to initialize all 20 members of SOPACE. The 1975-2016 climatology is used to calculate the monthly anomaly. (b) Box and whisker plot of AMOC trend (1979-2013) from LENS and SOPACE ensemble members. Orange lines show the median values, boxes show the middle 50% members, whiskers show the 5 to 95% members, and circles show the outliers.

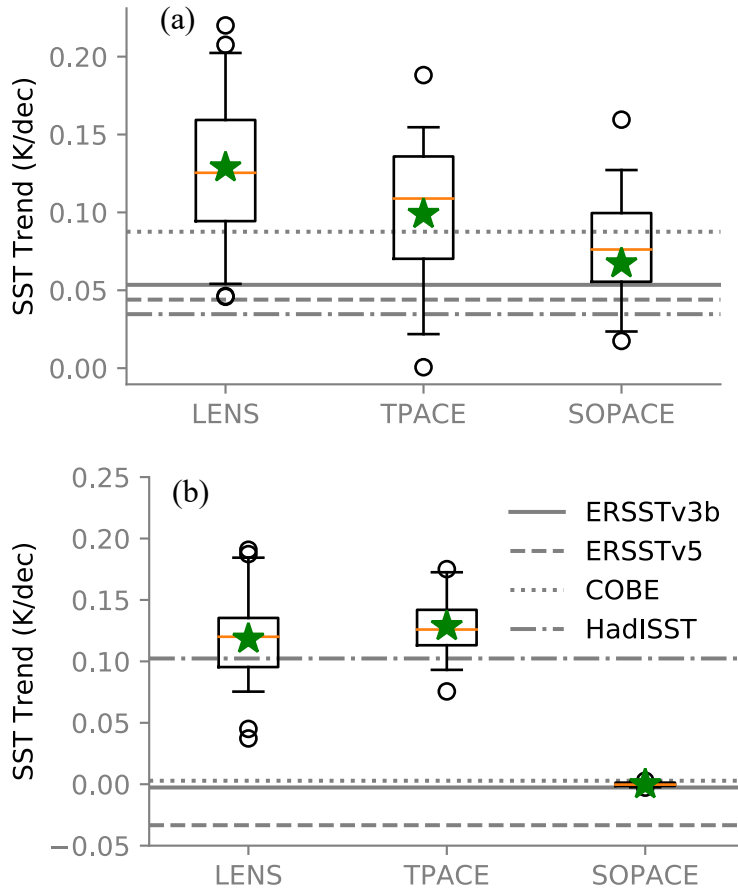


Figure S3. Box-and-whisker plot of SST trends averaged over (a) tropical South Atlantic (gray box in Figure 1f) and (b) the Southern Ocean (40S-65S) for each model ensemble. Green stars show the EM values. Orange lines show the median values. Gray horizontal lines show the observed values from various data sets: NOAA Extended Reconstruction SSTs version 3b and 5 (ERSSTv3b & ERSSTv5, Huang et al. 2017), Centennial in situ Observation-Based Estimates (COBE, Ishii et al. 2005), and the Hadley Centre Global Sea Ice and Sea Surface Temperature (HadISST, Rayner et al. 2003).

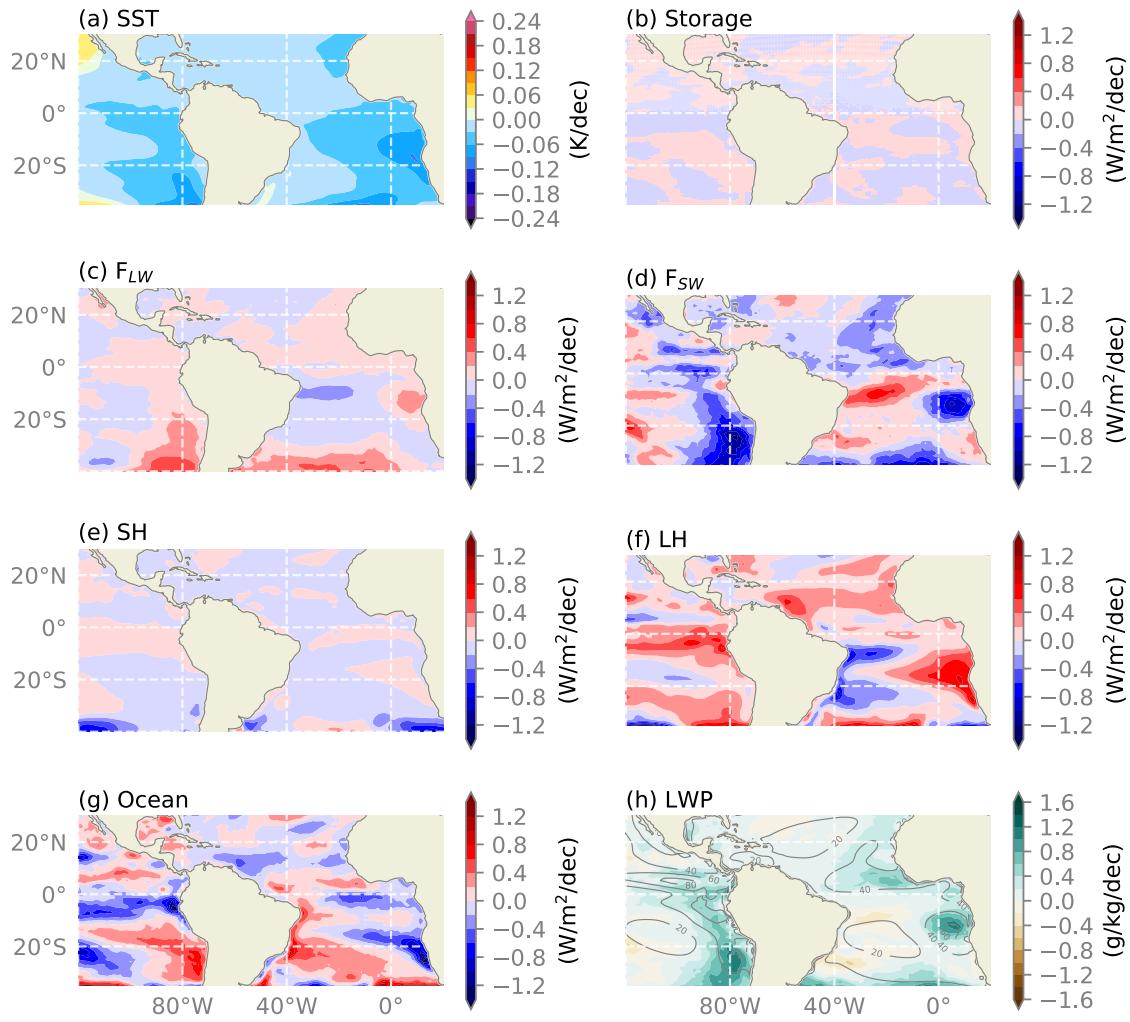


Figure S4. Terms in the ocean mixed layer heat budget based on monthly trends during 1979–2013 from SOPACE-internal over the tropical eastern Pacific and Atlantic. (a) SST trend, (b) trend in mixed layer heat storage (left hand side of equation (1)), (c) net longwave flux trend, (d) net shortwave flux trend, (e) sensible heat flux trend, (f) latent heat flux trend, (g) trend due to ocean dynamics, and (h) trend in liquid water path (contours show the climatological LWP). Positive flux is downward and warms the SST.

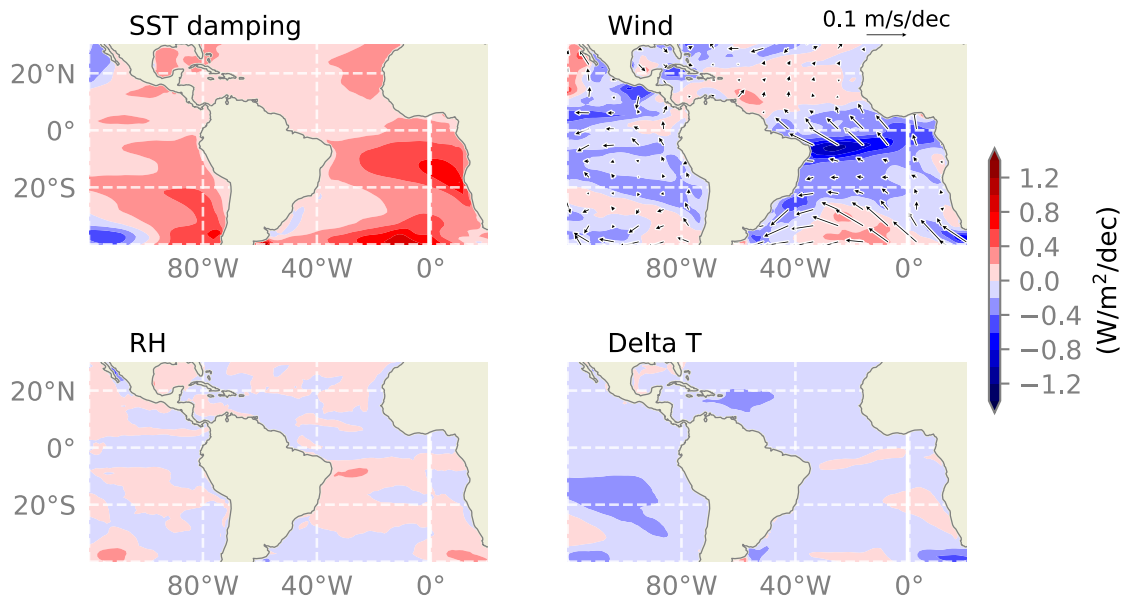


Figure S5. Latent heat budget based on monthly trends during 1979–2013 from SOPACE-internal over the tropical eastern Pacific and Atlantic due to (a) SST damping, (b) near-surface wind speed changes, (c) near-surface relative humidity changes, and (d) air-sea temperature difference changes. See Equation S6 for details.

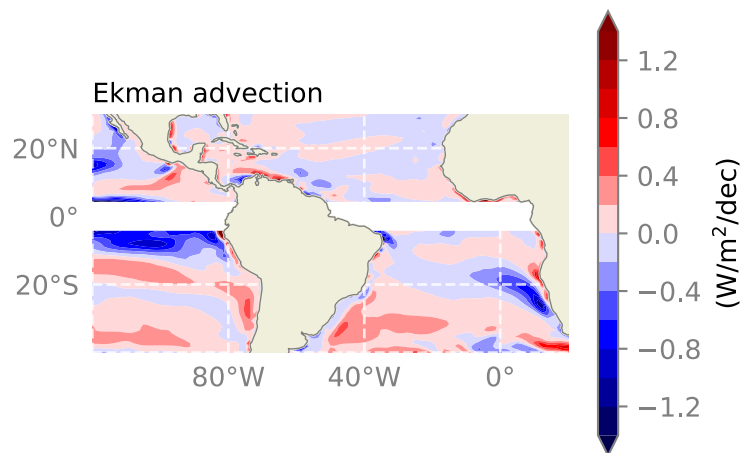


Figure S6. Ekman advection based on monthly trends during 1979–2013 from SOPACE-internal over the tropical eastern Pacific and Atlantic, expressed as an equivalent surface heat flux trend. Area near the equator (5°S–5°N) is masked out.